Post-Fire Damage Geospatial Assessment via Point Clouds of a Highway Bridge Structure

Yijun Liao[1], Mohammad Ebrahim Mohammadi[2], Richard L. Wood[3], and Christine E. Wittich[4]

[1] Dept. of Civil Engineering, University of Nebraska-Lincoln, Lincoln, NE, yijun.liao419@huskers.unl.edu
[2] Dept. of Civil Engineering, University of Nebraska-Lincoln, Lincoln, NE, me.m@huskers.unl.edu
[3] Dept. of Civil Engineering, University of Nebraska-Lincoln, Lincoln, NE, rwood@unl.edu
[4] Dept. of Civil Engineering, University of Nebraska-Lincoln, Lincoln, NE, cwittich@unl.edu

ABSTRACT: This paper discusses the quantitative post-fire damage assessment of a steel girder bridge via point clouds. In this case study, the point cloud was collected using light detection and ranging (lidar) for a detailed geometric and shape analysis. The out-of-plane deformation was analyzed to locate and quantify buckling across the length of the steel girders.

Test Structure and Measured Data

On Friday, June 1st, 2018, a vehicle caught fire on the I-80 westbound shoulder directly adjacent to the north side of the pier of the 10th street bridge in Omaha, Nebraska. The fire caused damage to the I-80 westbound pavement, barrier rail, north face of the bridge pier, steel girders and cross-frames of the superstructure, bridge deck, and utilities attached to the bridge (Figure 1a). Visual assessment was conducted following the event with observations including out-of-plane buckling of the steel girders as well as spalling and cracking of the concrete deck and pier. However, the visual damage assessment was not able to quantify the various damage patterns, nor indicate the extents of the damage along the girders due to the complex geometry of the structure [1]. Therefore, this study collected detailed geometric data using light detection and ranging (lidar) technology to analyze the complex buckling patterns of the bridge girders guide possible interventions.

SHM Methodology and Results

The data was collected using two lidar scanners: 1) Faro Focus 3D X-130, which has a range of 1.96 – 426.5 feet and a ranging error of ± 0.079 inches at 32.8 feet; and, 2) Faro Focus 3D S-350, which has a range of 1.96 – 1148 feet and a ranging error of ± 0.039 inches at 32.8 feet. A total of 33 scans were collected to achieve a high level of accuracy and maximize the coverage between individual girders and cross-frames. The individual lidar scans were registered to a single coordinate system with a mean alignment error of 0.072 inches. The root-mean-square error of the mean alignment is 0.061 inches and the point cloud is compiled to meet 0.099 inch (3D) accuracy at 95% confidence level, in accordance with guidelines specified by the Federal Geographic Data Committee [2]. The overview of the registered point cloud is displayed in Figure 1b.

To verify the accuracy of the collected point clouds, a quality control process was undertaken in which critical dimensions of the bridge were measured in the point clouds and compared to known values (from construction drawings). The critical dimensions for verification included: 1) the depth of the web of the eastmost girder at the center of the pier, and 2) the depth of the web of the same girder at the field splice in the westbound lanes. This girder was selected for the quality control process due to its proximity to the fire and the anticipated damage. The point cloud girder measurements are 81.41 inches and 56.53 inches as compared to known values of 81.37 inches and 56.50 inches from the bridge plans. This resulted in differences within 0.04 inch, which is less than the specified error of the lidar scanning platform.

(a)   (b)

Figure 1. The case study structure: (a) bridge view including lidar scanners deployed for point cloud collection, and (b) isometric view of aligned point cloud.

The out-of-plane deformation of select girder webs was analyzed via a depth-map approach. This was performed using a single point cloud that eliminates the registration error. An out-of-plane depth-map analysis enables each vertex of the point cloud to be classified based on its distance from a reference plane [3], as shown in Figure 2. In this case, the reference plane coincides with the plane of the girder's web, where positive out-of-plane deformation values are oriented eastbound and negative deformation values are oriented westbound. The depth-map analysis classified the deformation of the web up to one-hundredth of an inch, which is presented visually by color at the same resolution. In addition, the measurements of range, maximum, minimum, and median out-of-plane deformation values for each girder (at 99% to minimize any remaining noise) are identified in Table *1*. The out-of-plane deformation values are reported as a range value to indicate the amount of potential bucking or the lack of planarity in the girders.

Table 1. Maximum, minimum, median and range out-of-plane deformation values for girders.

Girder I.D.	Westbound (inch)				Eastbound (inch)			
	Min.	Max.	Median	Range	Min.	Max.	Median	Range
Eastmost	-1.09	1.20	-0.02	2.29	-0.74	0.43	-0.02	1.17
2nd Eastmost	-1.15	1.11	-0.01	2.26	-0.61	0.28	0.01	0.89

The visualization of the depth-map analysis enables the identification of the locations of maximum and minimum out-of-plane-deformation as well as its distribution throughout the girder web. As shown in Figure 2, the two girders underwent a severe deformation due to the elevated temperatures, where they experienced a total deformation (range from the minimum to the maximum) in excess of 2.2 inches approximately at the distance of 3.5 ft from the pier, respectively. In addition, the depth-map visualization indicates that second eastmost sustained additional localized deformations with maximum magnitudes in excess of 1.1 inches throughout its length up to the field splice in both out-of-plane directions. The eastmost girder sustained a localized out-of-plane deformation with a maximum magnitude of 1.2 inches, with respect to the reference plane, in the vicinity of the pier with additional localized deformation near the field splice. Similar analysis and results were detailed on other girders in both the eastbound and westbound lanes as well as select cross-frames [1].
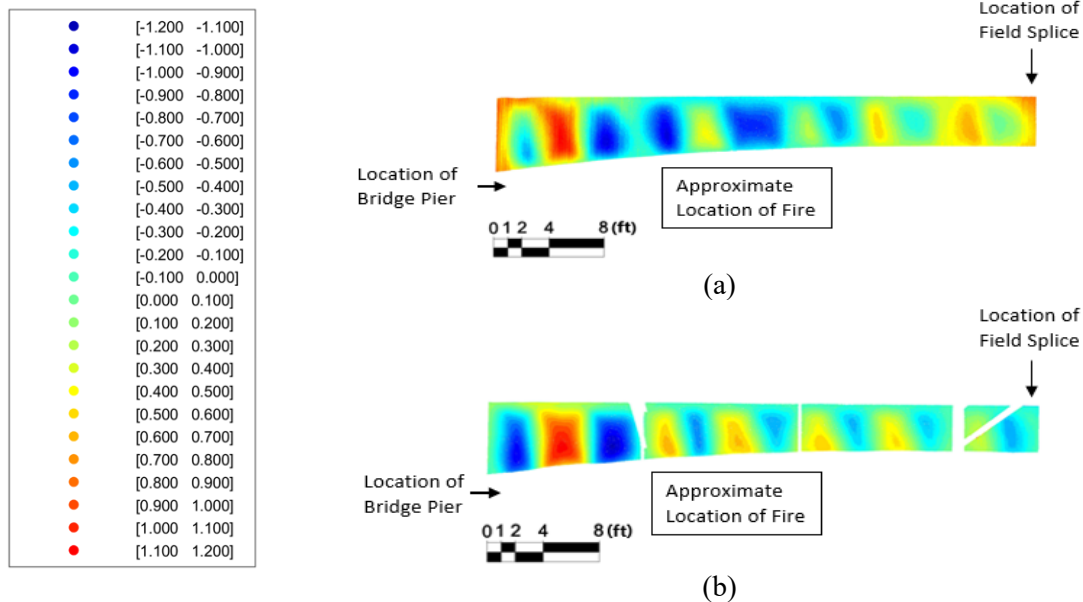
Figure 2. Depth map analysis results (in inches) on the westbound span (a) eastmost girder, (b) second eastmost girder.

Lessons Learned

Point clouds are an emerging data format that can be widely applied to various infrastructure. This case study presents the precise quantification of the out-of-plane deformation of bridge girders to monitor steel buckling for potential intervention. Buckling behavior as small as 0.1 in was evident in the depth maps, indicating the applicability of this approach for a variety of buckling monitoring scenarios. Based on this work and for precise quantification, it is recommended to use a single scan to avoid registration error, which introduces offsets even in tightly aligned point clouds. Furthermore, geometric information is observed to be most reliable since RGB information is inconclusive due to environmental effects (e.g., staining and power washing on the girders). Moreover, the depth map analysis incorporated only the lowest 99% of the points due to the presence of outlier points despite carefully applied filters. Inclusion of 100% of the points substantially reduces the resolution of the depth maps due to their low observed frequency of occurrence combined with the higher magnitudes of the highest 1%, which skews the color map.

Acknowledgements

References

[1] M.E. Mohammadi, Y. Liao, R.L. Wood, and C.E. Wittich. *Post-Fire Damage Geospatial Assessment of 10th Street Highway Bridge (S080 45433)*. Nebraska Transportation Center, University of Nebraska-Lincoln, Lincoln, Nebraska, 2019.

[2] Federal Geographic Data Committee (FGDC). Geospatial Positioning Accuracy Standards Part 3: National Standard for Spatial Data Accuracy. No. FGDC-STD-007.3-1998, USGS, Reston, Virginia.

[3] Shakarji, C. M. (1998). Least-squares fitting algorithms of the NIST algorithm testing system. *Journal of Research of the National Institute of Standards and Technology*, 103(6), 633.